Kinetic study of the pyrolysis of microalgae under nitrogen and CO2 atmosphere

Yu Hong, Chengrui Xie, Wanru Chen, Xiang Luo, Kaiqi Shi, Tao Wu

University of Nottingham
UK | CHINA | MALAYSIA

University of Nottingham Ningbo China, 199 Taikang East Road, Ningbo, 315100, China

First published 2019

University of Nottingham
UK | CHINA | MALAYSIA

Kinetic study of the pyrolysis of microalgae under nitrogen and CO_2 atmosphere

Yu Hong [a,d], Chengrui Xie [a], Wanru Chen [a], Xiang Luo [a,b], Kaiqi Shi [a,b], Tao Wu [b,c,*]

[a] Department of Chemical and Environmental Engineering, The University of Nottingham Ningbo China, Ningbo 315100, China

[b] New Materials Institute, The University of Nottingham Ningbo China, Ningbo 315100, China

[c] Municipal Key Laboratory of Clean Energy Conversion Technologies, The University of Nottingham Ningbo China, Ningbo 315100, China

[d] Research and Development Centre, Ningbo Thermal Power Co. Ltd., Ningbo 315040, PR China

Corresponding author: tao.wu@nottingham.ac.uk

Abstract

In this study, three primary components of algae (lipid, carbohydrate and protein) and one microalgae (spirulina) were pyrolyzed in a thermogravimetric analyzer (TGA) under nitrogen and CO_2 atmosphere at four heating rates. It was found that protein decomposed first, which was followed by carbohydrate and then lipid. Kinetic study revealed that ovalbumin (protein) had the lowest activation energy of ~70 kJ/mol for the initiation of pyrolysis. Oil droplet showed higher activation energy of 266.5 kJ/mol in CO_2 atmosphere, which suggests that algal lipid is more difficult to decompose in CO_2 atmosphere. However, for the pyrolysis of cellulose (carbohydrate), the activation energy (~310 kJ/mol) was similar under two different gas atmospheres tested. This study showed that CO_2 atmosphere favors the pyrolysis of algae with high protein content and low lipid content, since the existence of CO_2 promotes the cracking of VOCs as well as the reaction between VOCs and CO_2.

Keywords: Kinetics; Pyrolysis; Algae; Model compounds; Carbon dioxide

1 Introduction

As a renewable carbonaceous resource, marine biomass has recently attracted special interests and is regarded as a potential substituent to traditional fuels. The terrestrial biomass is primarily comprised of cellulose, hemicellulose and lignin [1], while algal biomass

consists of carbohydrates, proteins, and lipids, which has been investigated by many researchers on its conversion to various biofuels [2-6].

Two different approaches, i.e. thermogravimetric analysis (TGA) and differential thermogravimetric analysis (DTG), are commonly used to study the thermal decomposition of algae and its model components. Numerous research was focused on the thermal degradation of biomass via the observation of weight change with temperature [7-9]. Two commonly-used iso-conversional methods, i.e. Kissinger-Akahria-Sunose (KAS) and Flynn-Wall-Ozawa (FWO), were applied to conduct kinetic analysis of pyrolysis and thus to determine parameters including activation energy (E_a) and pre-exponential factor (A) [8, 10, 11]. However, the decomposition of different components in biomass leads to extremely complicated pyrolysis process, which makes the iso-conversional method relatively inappropriate [12]. More commonly, the model fitting method is used to simulate the kinetics of biomass pyrolysis by substituting different reaction models into Coats-Redfern function. The highest regression value of such indicates the best mechanism model for the pyrolysis event [13].

The conventional pyrolysis of biomass and the kinetic study have been discussed in many previous studies [8, 10, 12, 14-16]. It is reported that compared with N_2, the use of CO_2 as the carrier gas could assist the pyrolysis of carbonaceous materials and lead to some benefits such as higher thermal efficiency, reduced tar formation, higher production of syngas (especially CO), etc. [17, 18]. However, there is not much work that has been carried out on the kinetics of the pyrolysis of algal model compounds under carbon dioxide

50 atmosphere, as well as the comparison of the results produced under these two different
51 atmospheres.

52 In this study, kinetic study of the pyrolysis of three model compounds, i.e., carbohydrate,
53 lipid and protein, and microalgae- spirulina under N_2 and CO_2 atmospheres was conducted.
54 Iso-conversional method (Kissinger- Akahira-Sunose method) and model fitting method
55 (Coats-Redfern method) were applied to derive the activation energy (E_a) and pre-
56 exponential factor (A). The parameters and EDS analysis of the composition of char
57 obtained under N_2 and CO_2 atmosphere were also compared to reveal the pyrolysis of algae.

58 **2 Material and Methods**

59 **2.1 Materials**

60 Oil droplet (Optima 339 powdered vegetable fat), α- Cellulose ($(C_6H_{10}O_5)_n$, Aladdin®,
61 product code C104844) and ovalbumins (Sinopharm Chemical Reagent Co., Ltd, product
62 code 69003835) were selected to represent and simulate the pyrolysis of lipid,
63 carbohydrate, protein contents in algae, respectively, which followed the approach used by
64 other researchers [19-21]. Spirulina, the algae sample, was provided by Shandong Binzhou
65 Tianjian Biotechnology Co. Ltd. (Shandong Province, China). Raw materials were milled
66 (Retsch ZM200 Ultra-Centrifugal mill) and sieved to the same particle size of less than 120
67 μm.

2.2 Characterization of algae primary model compounds

The results of proximate, elemental and composition analyses are listed in **Error! Reference source not found.**, the procedure can be find in our previous studies [22-25]. The compositions of protein, lipid and carbohydrate in biomass were determined by Kjeldahl method (BS EN ISO 20483:2013), Soxhlet extraction (GB/T 5009.6-2003), and the difference calculated (GB/Z 21922-2008), respectively.

2.3 Kinetic analysis method

Pyrolysis of three algal pseudo-components and spirulina via conventional electric heating method was conducted on a thermogravimetric analyser (TGA, NETZSCH STA449F3, Germany) using non-isothermal process. Four different heating rates, i.e., 5, 10, 20 and 50°C/min, were used to heat the samples from 50 to 900 °C. The weight loss profile of each sample was subsequently derived. Pure nitrogen or carbon dioxide with a flowrate of 20mL/min was introduced into the system as carrier gas and to provide an oxygen-free atmosphere. The initial sample weight for each experiment was 2±0.5 mg. All experiments were repeated at least once to ensure accuracy and repeatability.

In order to investigate the effects of CO_2 on the carbon contained in solid residue, char samples were first prepared in a tube furnace (SG-GL1200K, Shanghai) using the same TGA heating programme, i.e. all samples were heated from 50 to 900 °C with a heating rate of 5 °C/min under a N_2 purge of 20 mL/min. The char samples collected were then subject to kinetic analysis (in CO_2) via the same procedure in TGA described previously.

2.3.1 Determination of Kinetic Parameters

The thermal decomposition of algae is a typical solid decomposition reaction, the rate of which is defined as Eq. (a),

$$\alpha = \frac{m_0 - m_T}{m_0 - m_f} \qquad \text{Eq. (a)}$$

Where m_0 is the initial mass of the material, m_f is the final mass of the solid material after pyrolysis, m_T is the mass of material at reaction temperature of T.

The kinetic study is based on the Arrhenius law. According to Eq. (a), the conversion rate only depends on the reaction temperature. The thermal dynamic formula can be described as Eq. (b),

$$\frac{d\alpha}{f(\alpha)} = \frac{A}{\beta}\exp\left(\frac{-E_a}{RT}\right)dT \qquad \text{Eq. (b)}$$

Where $f(\alpha)$ is the conversion (α)-dependent function; $\beta = \frac{dT}{dt}$ is the heating rate, K/min; E_a is the activation energy, J/mol; A is the pre-exponential factor, min^{-1}; R is the universal gas constant, 8.314 J/mol·K; T is the absolute temperature, K.

The integration of Eq. (b) over α is expressed as Eq. (c),

$$G(\alpha) = \int_0^{\alpha} \frac{d\alpha}{f(\alpha)} = \frac{A}{\beta}\int_0^{T} exp\left(\frac{-E_a}{RT}\right) dT \qquad \text{Eq. (c)}$$

Where $G(\alpha)$ is the integrated form of$f(\alpha)$.

2.3.2 Iso-conversional method: Kissinger- Akahira-Sunose (KAS)

Generally, the activation energy and pre-exponential factor of one-step fluid state reactions are constant, but these parameters would change depending on the conversion rate (α) for reactions involving solid, due to its internal heterogeneity of solid samples and complicated reaction mechanism [26]. Therefore, iso-conversional methods can be applied to determine the kinetic parameters of solid state reactions.

KAS method is based on Arrhenius equation using differential method [26, 27],

$$G(\alpha) = \frac{AE_a}{\beta R} p(\frac{E_a}{RT}) \qquad \text{Eq. (d)}$$

Combined with eq. (c), the variables of A, E_a and $f(\alpha)$ are related to T, whilst A and E_a are independent of α. Hence, Eq. (c) can be further integrated into the following form,

$$ln\frac{\beta}{T^2} = \ln\left(\frac{RA}{E_a G(\alpha)}\right) - \frac{E_a}{RT} \qquad \text{Eq. (e)}$$

The plot of $ln\frac{\beta}{T^2}$ versus $-\frac{1}{RT}$ for constant α will derive a linear relationship.

In order to reveal the correlation between E_a and α specifically, 19 conversion rates from 5 to 95% were selected. The E_a can be determined by the gradient of the linear profile.

2.3.3 Model fitting method: Coats-Redfern method

The Coats-Redfern method is one of the model fitting approaches, which can be used to calculate the kinetic parameters as well as to determine the order and mechanism of the reaction[28].

Coats-Redfern approximation was applied and further rearranged as Eq. (f),

$$ln\frac{G(\alpha)}{T^2} = \ln\left[\frac{AR}{\beta E_a}(1-\frac{2RT}{E_a})\right] - \frac{E_a}{RT} \quad \text{Eq. (f)}$$

The function $G(\alpha)$ depends on different reaction models [29].

The usual value of $\frac{2RT}{E_a}$ is far less than 1, which can normally be disregarded. Therefore, the equation could be simplified as Eq. (g),

$$ln\frac{G(\alpha)}{T^2} = \ln(\frac{AR}{\beta E_a}) - \frac{E_a}{RT} \quad \text{Eq. (g)}$$

By substituting different forms of $G(\alpha)$ into Eq. (g), a plot of $ln\frac{G(\alpha)}{T^2}$ versus $-\frac{1}{RT}$ is linear with a slope equal to E_a and the interception point provides values of E_a and A.

3 Results

3.1 Thermogravimetric analysis

Previous workers have examined single reaction model, and multiple parallel reaction model consisting up to seven-reactions based on different components or constituents in algae with different reactivity [30]. In previous study, ovalbumin [19], cellulose [20], and oil droplet [21] were used to represent protein, carbohydrate and lipid in algae, therefore, these compounds were chosen in this study to represent the protein, carbohydrate and lipid content in spirulina. The simulated TGA and DTG curves of spirulina were calculated using the sum of each TGA and DTG data of three model compounds multiplied to the corresponding composition of protein, carbohydrate, and lipid content in spirulina (**Error! Reference source not found.**).As shown in Figures 1 and 2, the use of these three components could simulate the actual alga with relatively satisfactory accuracy, the same as what was

142 reported by other researcher [31, 32]. Multiple pyrolysis of algal model compounds,

143 spirulina, and the calculated data for spirulina at heating rates of 5, 10, 20 and 50 °C/min

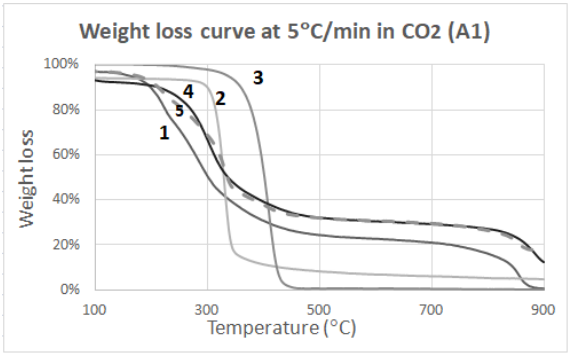

144 are illustrated in Figure 1 and

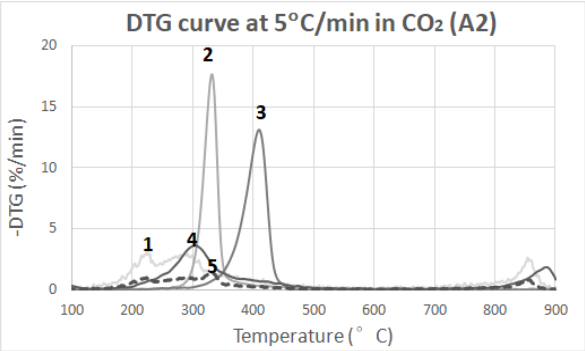

145

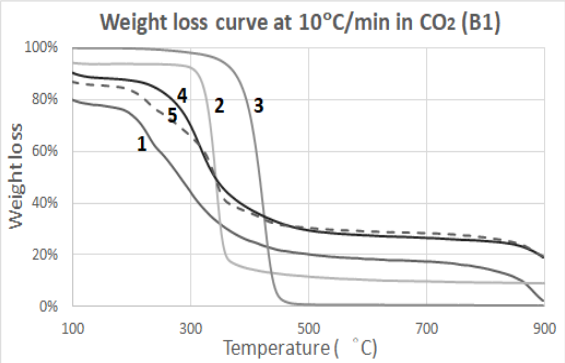

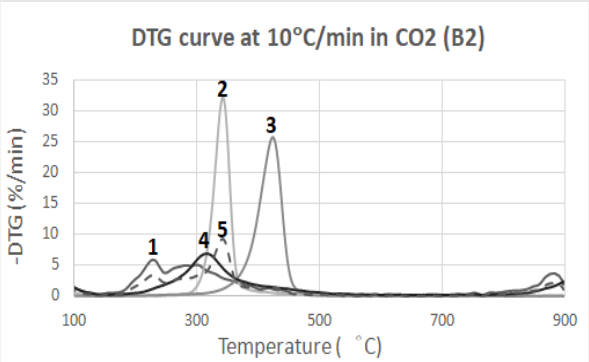

146

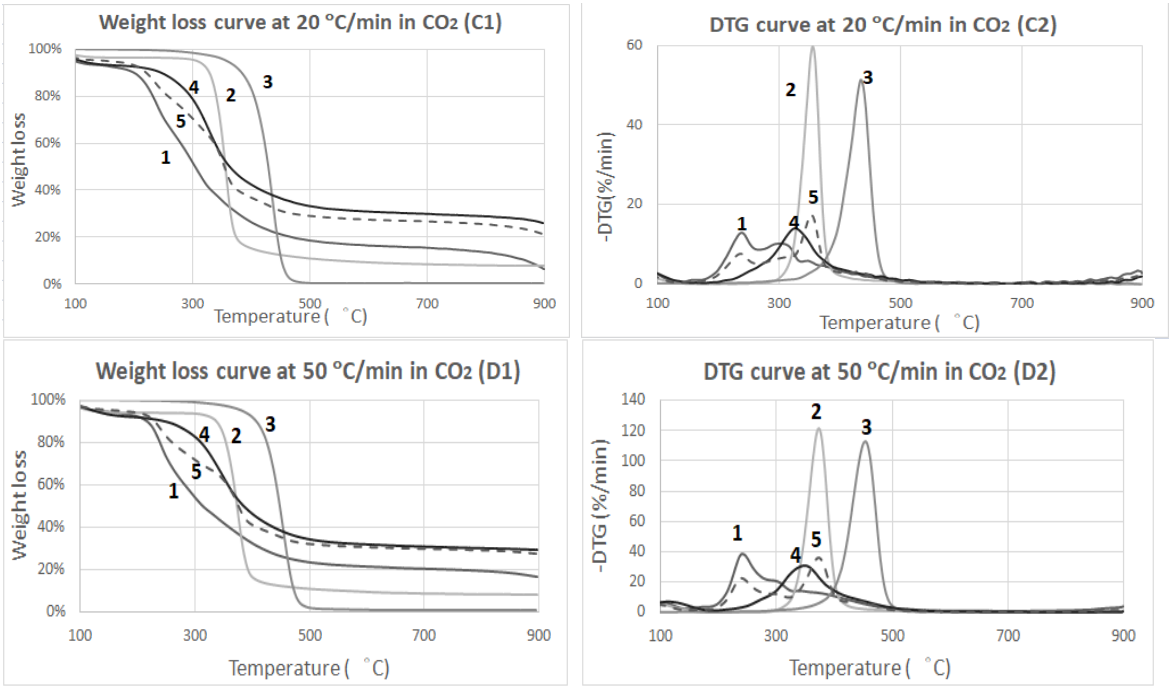

Figure 2, in order to reveal its mechanism [33]. Although the heating rates were different, the TG curves were comparable with similar initial and final temperatures. However, the peak value of DTG curve shifted to higher temperature zone as the heating rate increased and reached the set maximum of 50 °C/min. This phenomenon is attributed to the hysteresis in heat transfer from crucible to sample, as well as the difference in actual temperature of the samples and that of the measured temperature of the crucible. Moreover, the larger amount of volatile matter released with elevating heating rate. Apparent from the comparison of DTG curves under N_2 and CO_2, ovalbumin showed higher weight loss rate under CO_2, whilst the rate of weight loss for oil droplet and cellulose remained unchanged.

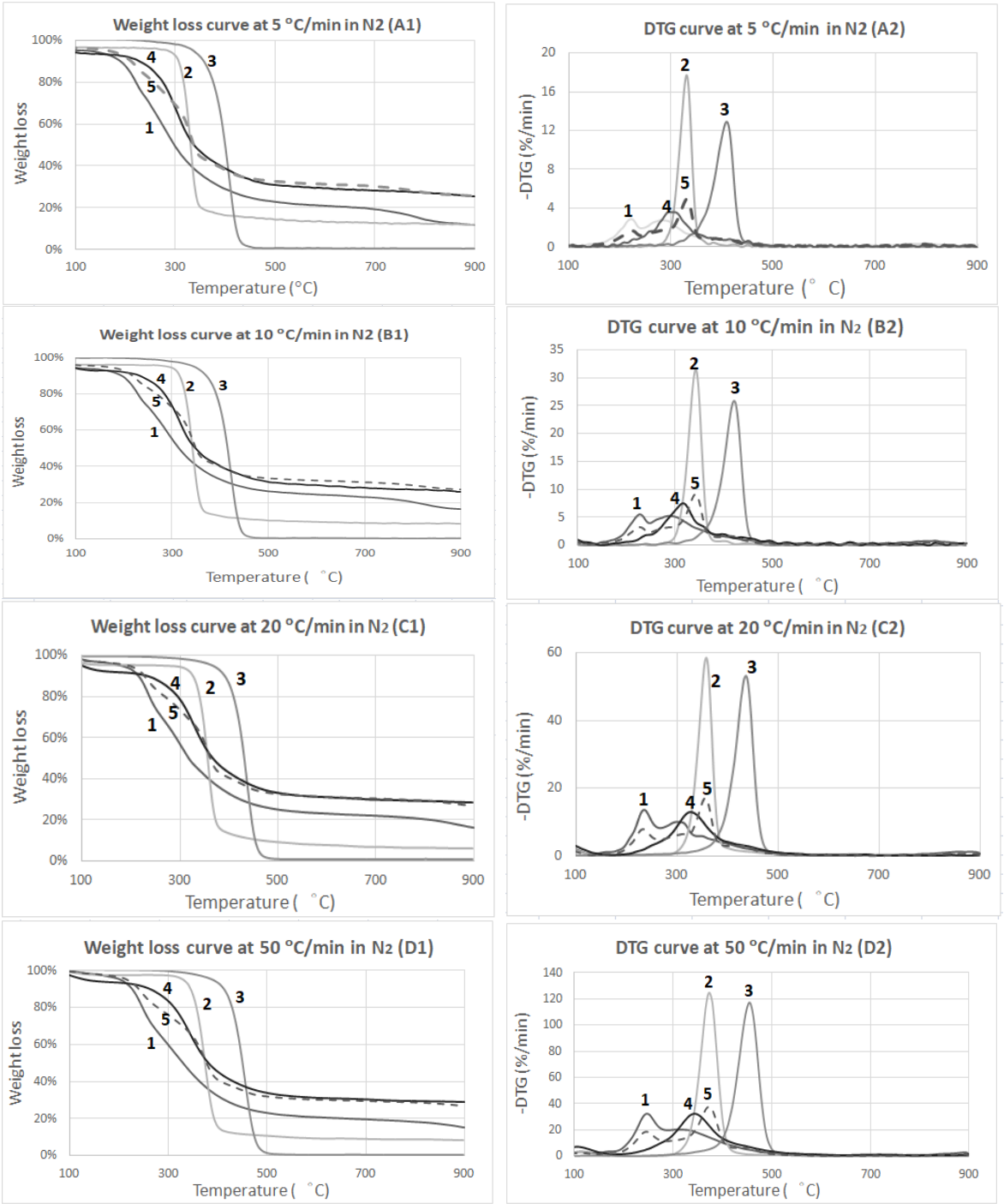

Figure 1 TG (1) and DTG (2) curves of the pyrolysis of ovalbumin (1), cellulose (2), oil droplet (3), spirulina (4) and simulative spirulina (5) under N_2 at different heating rates of 5 (A), 10 (B), 20 (C), and 50 (D) °C /min.

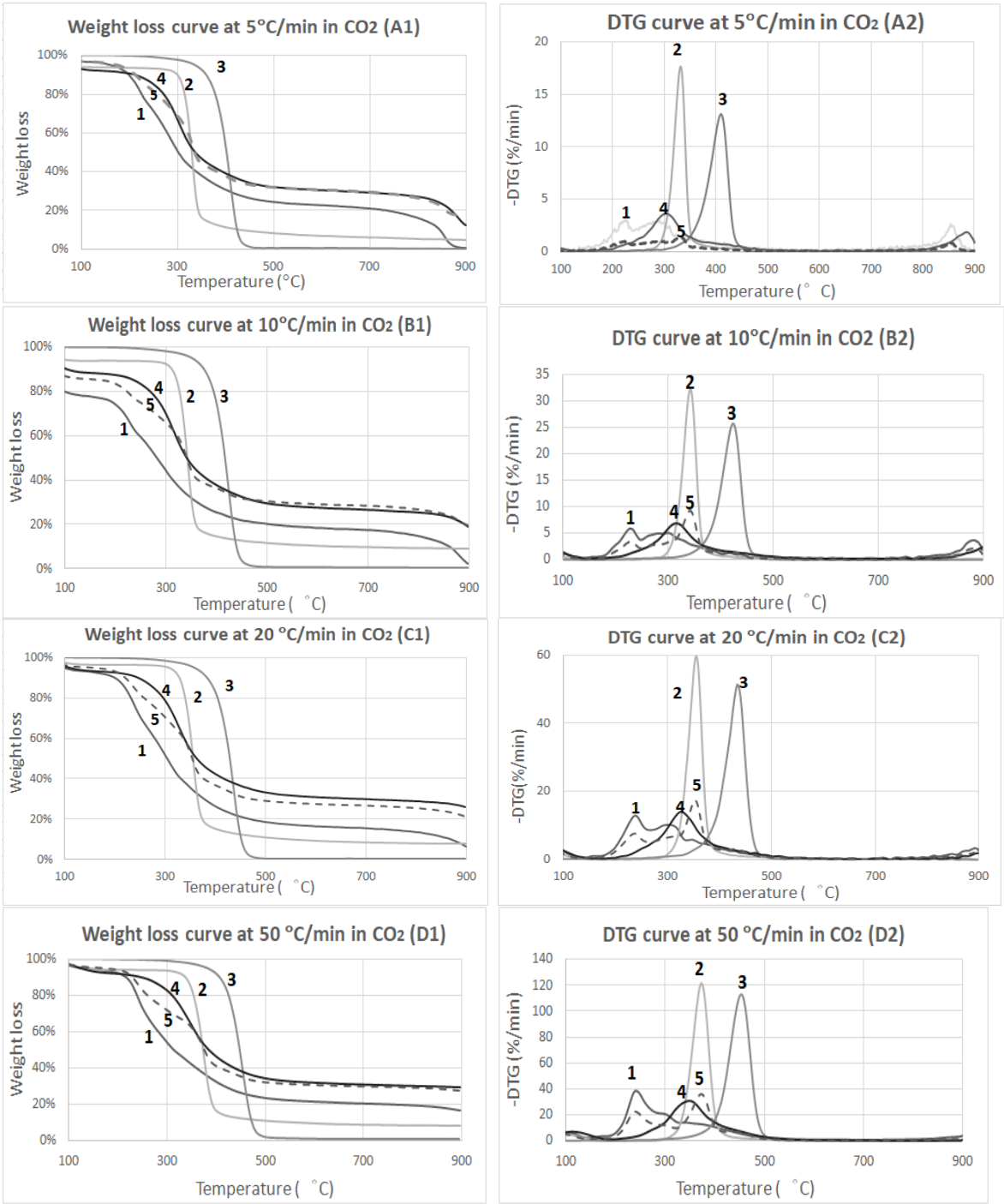

Figure 2 TG and DTG curves of the pyrolysis of ovalbumin (1), cellulose (2), oil droplet (3), spirulina (4) and simulativespirulina (5) under CO_2 at different heating rates of 5 (A), 10 (B), 20 (C), and 50 (D) °C /min.

Table 1 Characteristics of cellulose, ovalbumin, oil droplet and spirulina

	Ovalbumin	Cellulose	Oil droplet	Spirulina
Proximate analysis (wet basis, wt. %)				
Moisture content	2.0	2.7	0	6.7
Volatile matters	86.6	88.6	100.0	73.5
Fixed carbon	9.9	7.6	0	13.2
Ash content	0	1.1	0	6.6
Ultimate analysis (dry ash free basis, wt. %)				
C	41.6	42.7	75.8	49.8
H	7.0	6.5	11.8	6.6
N	12.2	0	0	11.0
S	1.2	0	0	0.7
O	38.0	50.8	12.4	31.9
HHV (MJ/kg)	18.73	16.99	39.07	20.55
Composition of sample (wt. %)				
Protein	81.6	0	0	57.8
Lipid	1.1	1.2	99.6	2.9
Carbohydrate	7.9	97.1	0.1	23.4

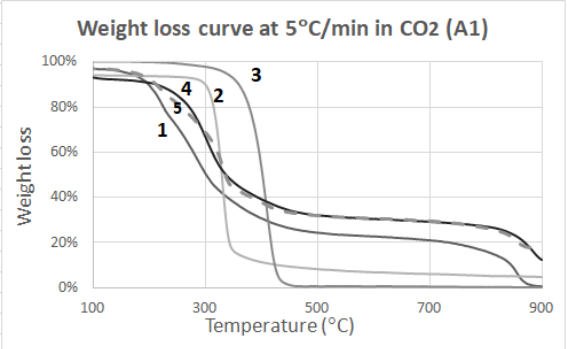

Figure 1 and

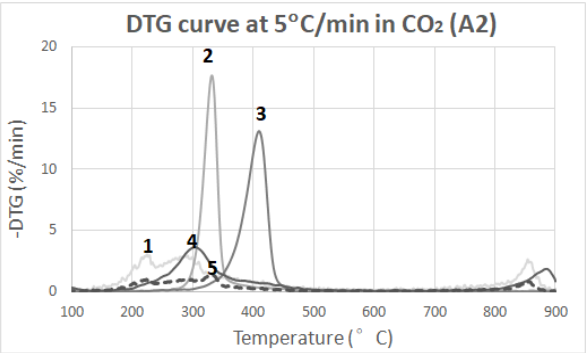

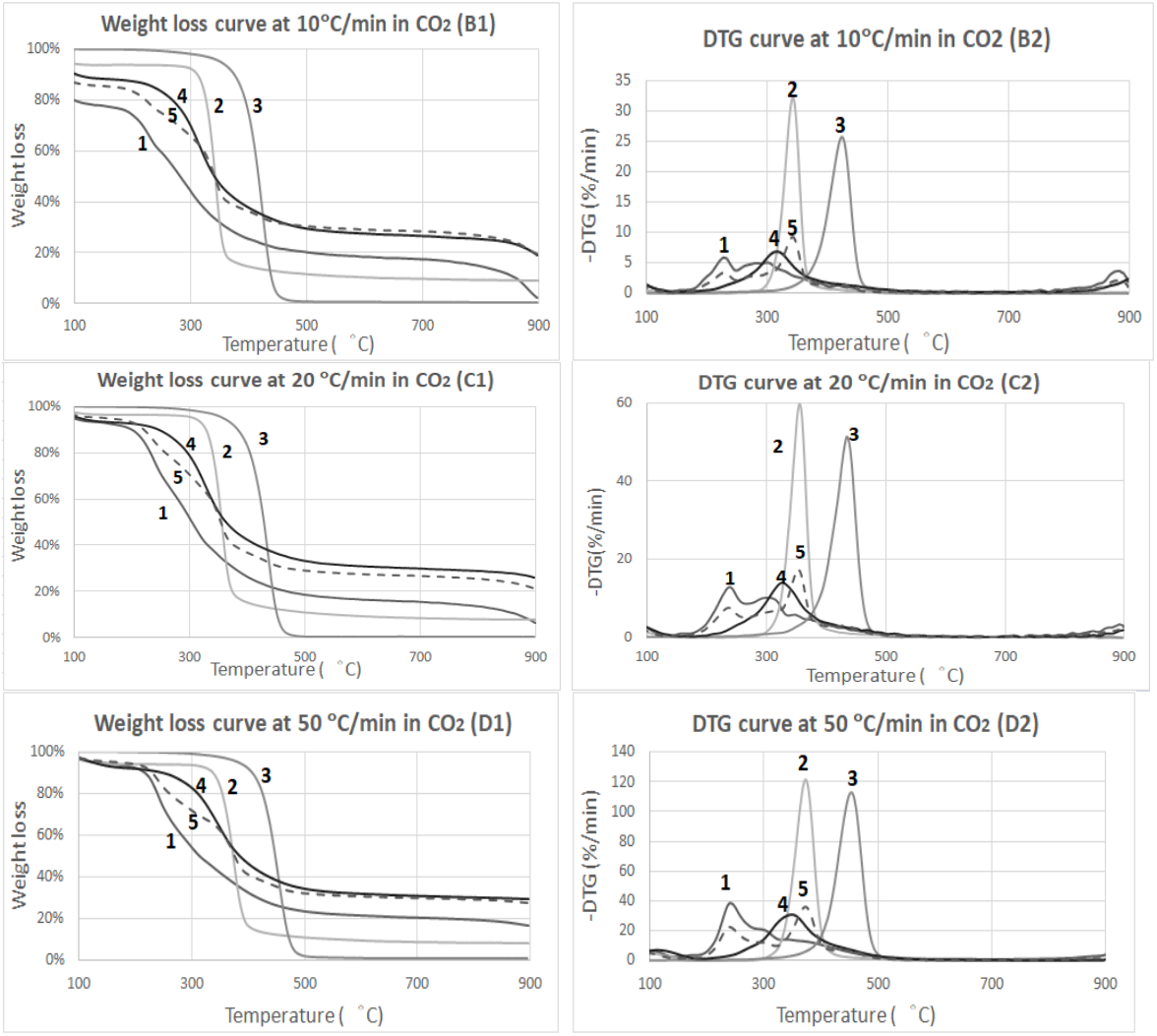

Figure 2 show that the degradation pattern of model compounds and algae were similar with three common stages involving dehydration, volatilization and carbonization under both N_2 and CO_2 atmospheres. The first stage started from ambient temperature to the temperature where light volatiles began to release, during which the moisture in biomass was removed at around 105°C. Although only slight weight loss has been observed during this stage, the structure of sample has changed. A major weight loss was recorded in the second stage ranging from 150 to 500°C, primarily due to the devolatilization of organic

matters. Ovalbumin, cellulose, oil droplet and spirulina decomposed mainly in the temperature range of 180-250, 290-370, 330-470 and 220-400°C, respectively. Given the low decomposition temperature, it can be inferred that the protein and carbohydrate of algae are of low thermal stability, whilst lipid is of high thermal stability under both atmospheres. This waste losst is regarded as the main pyrolysis stage. The third stage (500-800°C) showed a steady weight loss which was resulted from the decomposition of non-volatile carbonaceous residues. Char was formed whilst CO_2 and CO were removed [34, 35].

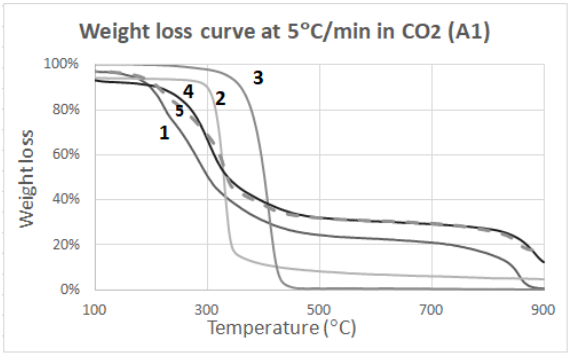

As evident from Figure 1 and

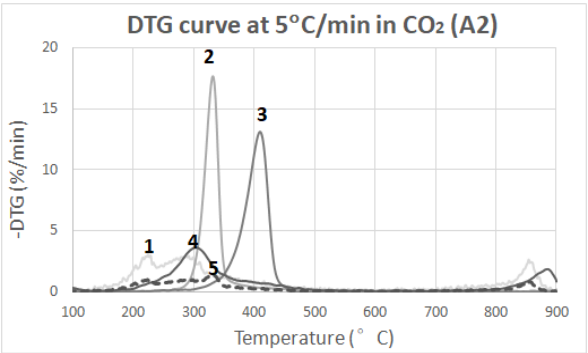

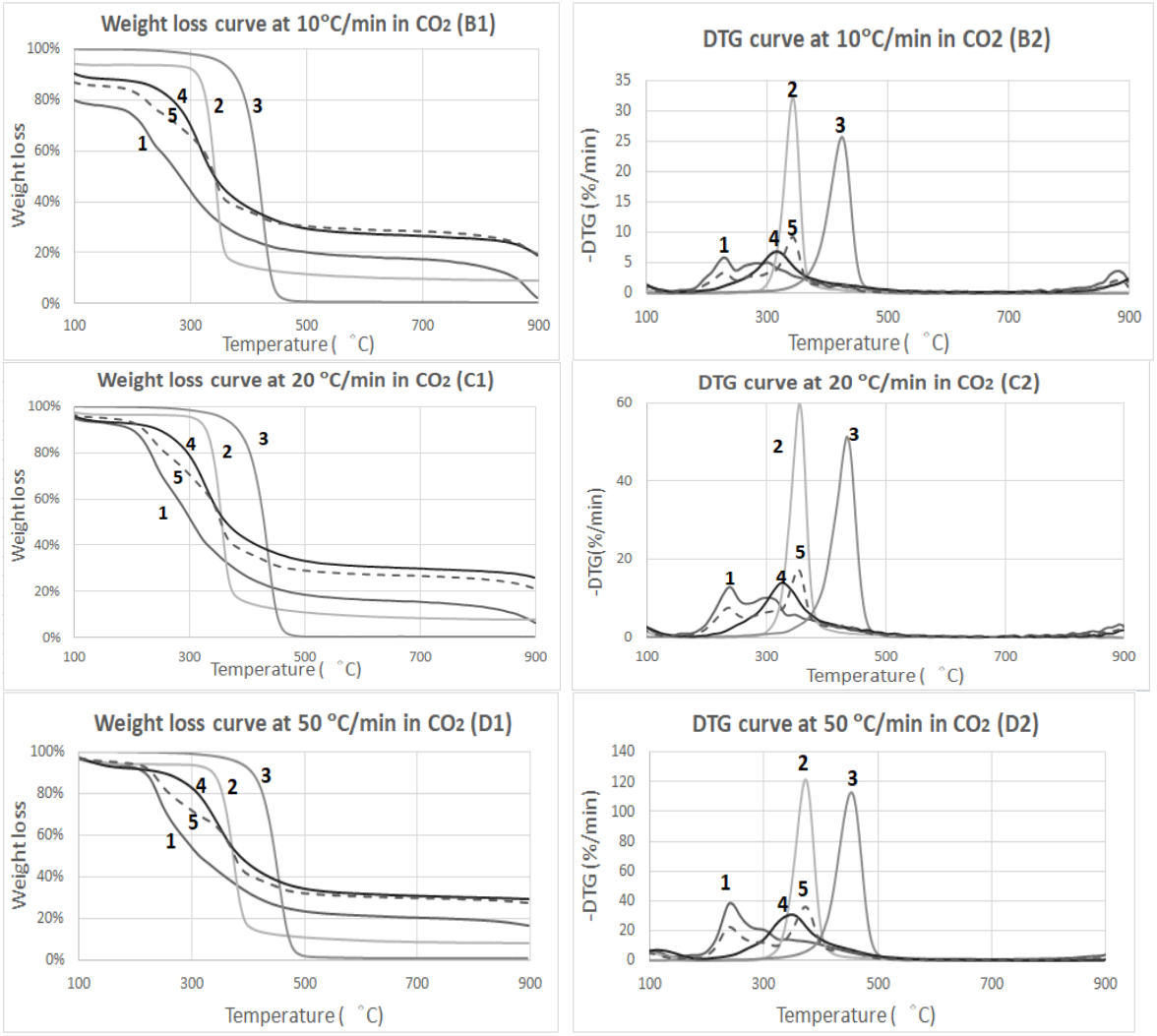

Figure 2, the TG curve of the model spirulina is relatively similar to that of the actual spirulina under both atmospheres. As for the DTG curves, the theoretical weight loss rate has two peak values, around 200 and 350°C under both atmospheres, which is similar to the DTG curve of the pyrolysis of ovalbumin. This is due to the excessive undefined substances contained in ovalbumin, rather than in spirulina. Therefore, the first peak in DTG curves of both spirulina and its model curve is attributed to those components that are not

within the scope of the model compounds. The second peak appeared at higher pyrolysis temperature with larger weight loss rate is likely associated with the thermal hysteresis.

The CO_2 gasification of carbon normally occurs more significantly at high temperature range above 800°C and leads to the significant consumption of carbonaceous residues [36]. Therefore, for comparison of the pyrolytic behavior under two different atmospheres, the lower temperature range of the TGA curves (100-800°C) is examined in this study. **Error! Reference source not found.** summarizes the primary pyrolysis parameters including Y_{char}, the weight percentage of char residue at 800°C; T_i, the initial temperature when volatile matters start to release; D_m, the maximum weight loss rate; T_m, the peak temperature; $\Delta T_{1/2}$, the half peak width temperature, which were all derived from TG and DTG curves (Figure 1 and

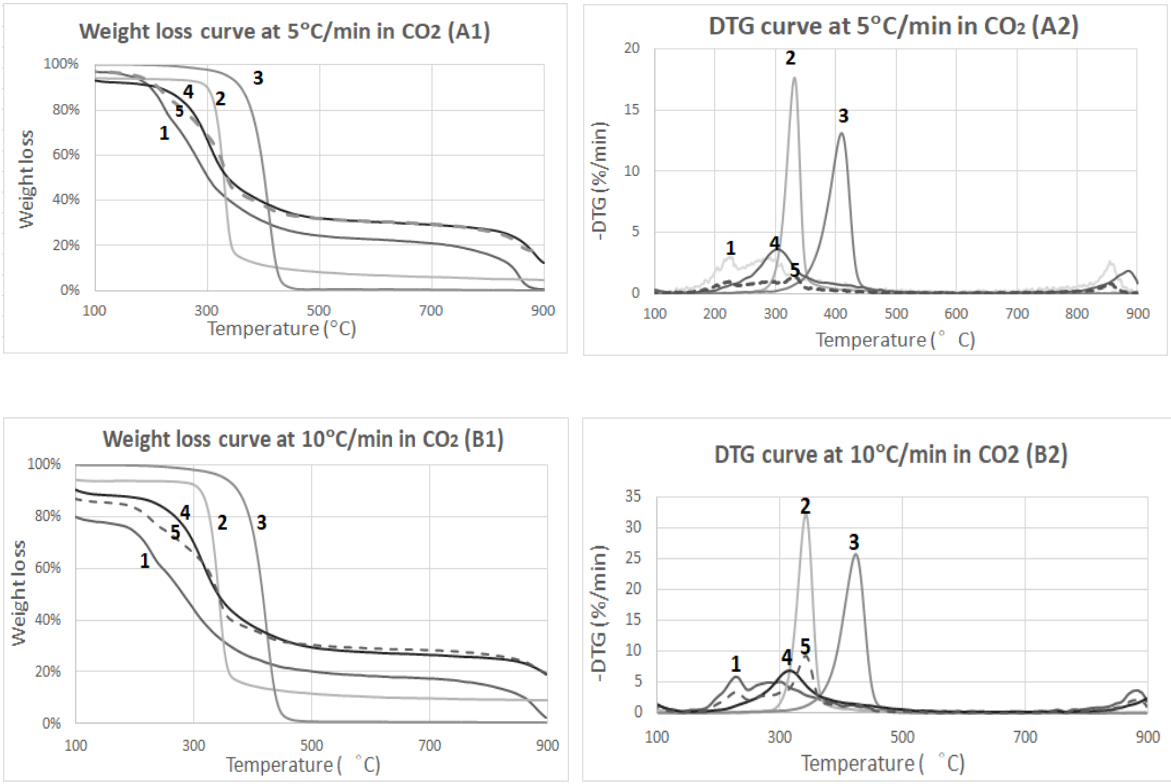

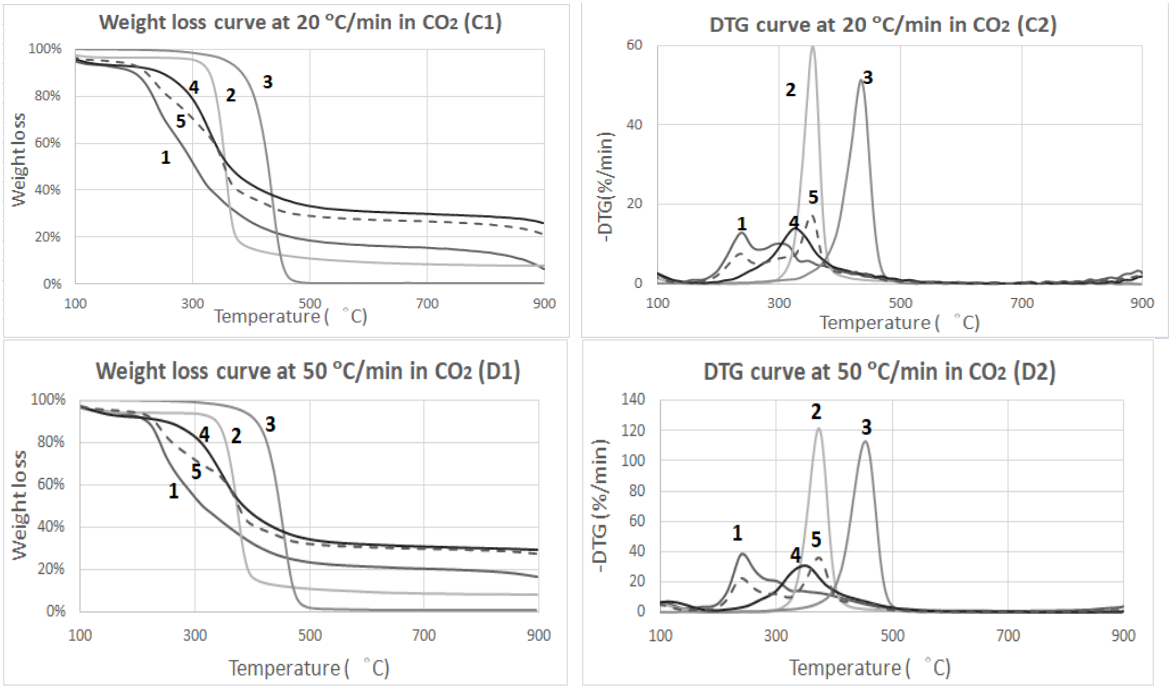

Figure 2). From **Error! Reference source not found.**, the char residue of oil droplet, cellulose, ovalbumin and spirulina after pyrolysis remained relatively unchanged under both atmospheres for the different heating rates. Due to the thermal hysteresis, D_m, T_m and T_i increased with increasing heating rate as observed in both atmospheres. It has been previously reported that the higher heating rate could reduce the reaction time and postpone the pyrolysis [37]. Moreover, according to a typical comparison of TGA curves between N_2 and CO_2 atmospheres (Figure 3), CO_2 assisted in the pyrolysis of ovalbumin and therefore the protein in algae, which shows a larger weight loss rate compared with that under N_2. However, the weight loss curves of cellulose and oil droplet pyrolysis derived in CO_2 stayed consistent with curves under N_2. This refers to the findings that CO_2 does not participate in the pyrolysis of carbohydrate and lipid contained in algae.

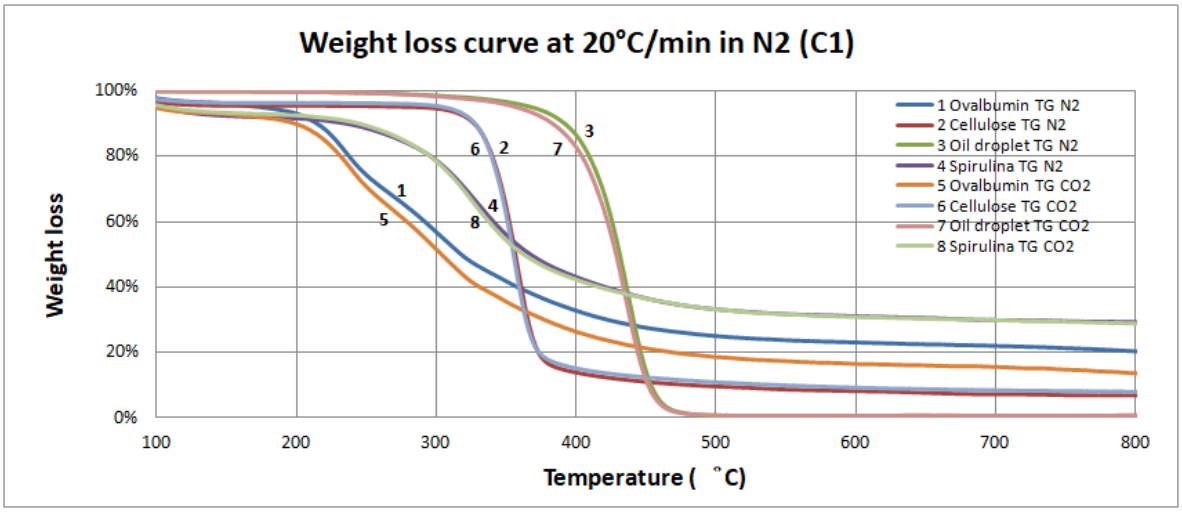

Figure 3 Weight loss curves of ovalbumin (1 and 5), cellulose (2 and6), oil droplet (3 and 7) and spirulina (4 and 8) at 20 C/min under N_2 and CO_2.

Table 2 Features of the pyrolysis of cellulose, ovalbumin, oil droplet and spirulina under N_2 and CO_2.

Sample		N_2				CO_2			
	β (°C min^{-1})	5	10	20	50	5	10	20	50
Ovalbumin	Y_{char} (%)	14.4	20.2	20.2	18.4	15.9	14.6	14.0	19.5
	T_i (°C)	186	193	197	208	187	197	202	214
	T_m (°C)	219	228	232	242	216	224	231	245
	D_m (%/min)	-2.3	-4.7	-9.7	-23.9	-2.3	-4.4	-9.0	-25.1
	$\Delta T_{1/2}$(°C)	78	92	123	137	87	93	98	140
Cellulose	Y_{char} (%)	12.1	8.6	6.6	8.8	5.4	9.3	8.1	8.7
	T_i (°C)	299	309	319	330	297	289	318	330
	T_m (°C)	326	338	349	364	325	338	350	364
	D_m (%/min)	-13.6	-25.2	-47.4	-100.1	-13.9	-25.5	-47.8	-101.5
	$\Delta T_{1/2}$(°C)	67	85	125	176	67	81	90	143
Oil droplet	Y_{char} (%)	0.5	0.5	0.7	0.7	0.4	0.6	0.7	0.9
	T_i (°C)	240	255	261	274	209	223	226	233
	T_m (°C)	410	422	437	455	410	423	435	449
	D_m (%/min)	-13.5	-25.9	-53.0	-114.2	-13.1	-25.7	-51.4	-115.0
	$\Delta T_{1/2}$(°C)	91	106	114	135	108	119	115	107
Spirulina	Y_{char} (%)	27.0	27.0	29.2	29.6	27.0	25.5	28.7	30.1
	T_i (°C)	225	235	243	255	227	236	243	254
	T_m (°C)	300	310	322	338	296	306	322	337
	D_m (%/min)	-2.9	-5.8	-11.5	-27.6	-2.8	-5.8	-10.9	-24.8
	$\Delta T_{1/2}$(°C)	125	146	169	192	131	143	178	194

** Y_{char} is the weight percentage of char residue at 800°C; T_i is the initial temperature when volatile matters start to release; D_m is the maximum weight loss rate; T_m is the peak temperature; $\Delta T_{1/2}$ is the half peak width temperature.*

3.2 Kinetic study

3.2.1 Determination of activation energy via Kissinger- Akahira-Sunose (KAS)

Amongst the three stages of pyrolysis, the second stage-devolatilization is regarded as the major step in algae decomposition, and thus the main scope of study. Based on the starting and finishing temperatures, under both atmospheres, ovalbumin was the first to decompose at around 180°C and sustained until 600°C at which the weight loss rate was nearly zero. Cellulose was the second to pyrolyze at around 250 - 500°C and oil droplet was the last to initiate its pyrolysis at 300°C and finishing at around 550°C. As a result of the synergistic effect of protein, carbohydrate and lipid in algae, the actual spirulina decomposed within a smaller temperature range, but still within the decomposition range of the three individual components, at around 220°C and terminating at 420°C. Therefore, after considering the pyrolysis of all four samples, temperature range for applying KAS method was selected as 120 to 600°C, which covered the temperatures of the whole conversion process.

In order to study the dependence of activation energy of model compounds on the increasing conversion rate (α), 19 different conversion rates from 5% to 95% at 5% intervals were investigated at four heating rates of 5, 10, 20 and 50 °C/min under N_2 and CO_2 based on KAS method. The activation energy (E_a) and correlation factor (R^2) of model compounds are listed in **Error! Reference source not found.**. Generally, due to the delay of heat transfer from pan to sample, the thermal delay was inherited into the process as the evident from the shift of DTG peak values towards higher temperature zone as the heating rate increased.

265 The activation energy derived, via KAS method, during the main stage of pyrolysis is of
266 sufficient accuracy and can be deployed for analysis [38]. Moreover, the R^2 values derived
267 for this stage are mostly above 0.90, which indicates the reliability of the calculated E_a.
268 However, the initial and final stages of sample conversion might contain unavoidable errors
269 due to the compositional heterogeneity of solid sample and experimental errors [39, 40].
270 Figure 4 shows the plot of activation energy obtained from KAS method against the
271 conversion rate under N_2 and CO_2 atmosphere for the pyrolysis of model compounds and
272 actual algae.

273

Table 3 The activation energy (E_a, kJ/mol) and correlation factor (R^2) of model compounds and spirulina under N_2 and CO_2 at different conversion rate (α) using KAS method.

N_2								
	Ovalbumin		**α-Cellulose**		**Oil droplet**		**Spirulina**	
α	E_a	R^2	E_a	R^2	E_a	R^2	E_a	R^2
5%	188.4	0.9880	202.5	0.9915	123.1	0.9323	162.5	0.9978
10%	202.4	0.9881	198.9	0.9963	136.1	0.9763	177.5	0.9987
15%	209.7	0.9892	196.2	0.9970	147.0	0.9905	183.2	0.9996
20%	209.9	0.9836	194.7	0.9972	154.9	0.9934	183.0	0.9998
25%	231.6	0.9920	193.6	0.9974	163.2	0.9965	182.2	0.9997
30%	232.0	0.9921	191.7	0.9977	166.0	0.9973	182.1	0.9998
35%	234.6	0.9808	189.9	0.9979	169.8	0.9979	182.0	0.9997
40%	237.9	0.9654	188.1	0.9982	173.0	0.9981	182.6	0.9995
45%	237.9	0.9675	186.8	0.9984	175.2	0.9987	183.9	0.9990
50%	233.4	0.9696	185.6	0.9984	186.1	0.9936	186.8	0.9985
55%	231.7	0.9658	184.5	0.9985	189.6	0.9920	191.2	0.9974
60%	240.8	0.9490	182.9	0.9987	183.0	0.9980	200.0	0.9956
65%	255.0	0.9195	181.0	0.9990	179.5	0.9988	218.0	0.9914
70%	278.5	0.8695	179.3	0.9990	180.9	0.9987	249.2	0.9842
75%	331.6	0.7119	178.2	0.9992	182.1	0.9985	299.5	0.9436
80%	165.2	0.1812	176.2	0.9992	183.6	0.9986	335.5	0.9228
85%	-29.8	0.0157	174.1	0.9994	183.6	0.9985	305.7	0.8717
90%	-64.7	0.3252	171.4	0.9994	185.3	0.9980	203.2	0.4713
95%	334.3	0.6023	167.7	0.7146	180.6	0.9972	28.8	0.0255
CO_2								
	Ovalbumin		**α-Cellulose**		**Oil droplet**		**Spirulina**	
α	E_a	R^2	E_a	R^2	E_a	R^2	E_a	R^2
5%	148.9	0.9820	187.6	0.9975	156.9	0.9918	178.1	0.9981
10%	183.8	0.9844	189.9	0.9777	168.6	0.9945	218.4	0.9976
15%	202.3	0.9838	187.1	0.9955	173.8	0.9957	233.2	0.9996
20%	231.5	0.9698	183.6	0.9980	181.1	0.9962	234.9	0.9978
25%	315.0	0.9291	180.6	0.9985	184.4	0.9959	235.2	0.9957
30%	376.4	0.8623	178.5	0.9988	188.5	0.9960	237.6	0.9924
35%	420.8	0.8267	177.6	0.9987	192.5	0.9962	243.6	0.9883
40%	462.5	0.7931	175.6	0.9988	193.4	0.9970	255.5	0.9776
45%	504.4	0.7552	174.7	0.9990	197.3	0.9967	278.2	0.9533
50%	572.0	0.6446	173.6	0.9990	198.6	0.9971	314.7	0.8680
55%	298.5	0.0759	172.5	0.9993	199.6	0.9975	316.7	0.5007
60%	-485.6	0.5018	172.2	0.9994	202.2	0.9973	-52.2	0.0139
65%	-291.7	0.8597	172.0	0.9995	203.7	0.9975	-182.0	0.4655
70%	-168.0	0.9059	171.7	0.9997	204.2	0.9977	-147.9	0.7375
75%	-96.8	0.9426	170.9	0.9999	205.1	0.9978	-97.0	0.8374
80%	-47.0	0.9233	170.4	1.0000	206.0	0.9980	-45.8	0.8669
85%	-53.3	0.9153	171.5	1.0000	206.4	0.9981	-43.8	0.9261
90%	-88.1	0.7844	179.0	0.9998	208.0	0.9977	-47.4	0.9196
95%	-205.3	0.1403	342.8	0.2799	209.5	0.9984	-75.2	0.8890

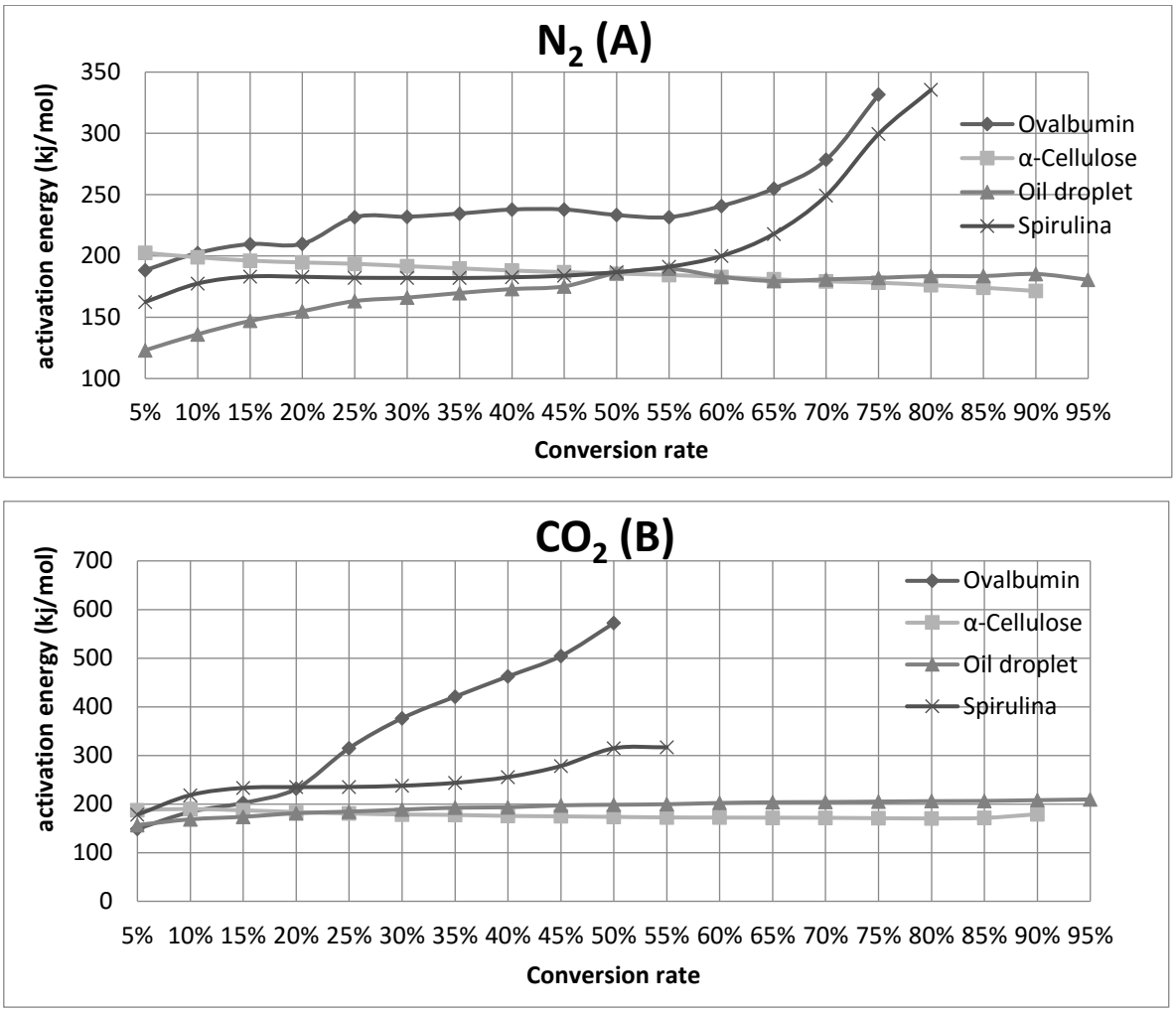

Figure 4 The activation energy of ovalbumin, cellulose, oil droplet and spirulina against the conversion rate under N_2 (A) and CO_2 (B)

It is noticed that E_a of three model compounds varied along with the increment of conversion rate. The E_a of oil droplet increased gradually from 123.1 to 175.2 kJ/mol within the conversion range of 5 to 45%, after which it remained relatively unchanged starting from around 180 kJ/mol in N_2. Similarly, when CO_2 was used, E_a of oil droplet progressively increased from 156.9 to 197.3 kJ/mol within the conversion rate of 5-45%, while that value

288 fluctuated at round 200 kJ/mol from 50 to 95% conversion. The E_a values were 5.3-27.5%
289 larger than those derived in N_2, which suggested that the lipid content in algae is relatively
290 more stable and difficult to decompose under CO_2 atmosphere. The results agreed with the
291 initial test at the beginning of pyrolysis where oil droplet showed the highest activation
292 energy amongst the three model compounds, which was corresponding to the order of T_i
293 values in TG analysis.

294 A contrary trend was found in the pyrolysis of cellulose under N_2 atmosphere, where the
295 activation energy reduced gradually from 202.5 to 171.4 kJ/mol for the conversion of 5 to
296 90%. As for the pyrolysis of cellulose in CO_2, the activation energy also decreased from 187.6
297 to 171.5 kJ/mol for the same conversion range. According to Figure 4, a slightly lower
298 activation energy was recorded for the decomposition of cellulose under CO_2, in
299 comparison with the energy calculated using N_2 as the carrier gas. This is in opposite to that
300 found in lipid pyrolysis.

301 As for the ovalbumin, the activation energy increased from 188.4 to 209.9 kJ/mol when the
302 conversion (α) increased from 5 to 20%. It increased slightly to 230 kJ/mol when the
303 conversion further increased to 55% and peaked at 331.6 kJ/mol when conversion was 75%.
304 E_a values could be ignored beyond the conversion rate of 80%, which mainly caused by the
305 crossover of TG weight loss curve resulted from the heterogeneous nature in composition
306 of solid sample [41]. However, the activation energy distribution indicated a different
307 pattern in CO_2. The energy required increased significantly from 148.9 to 572 kJ/mol for the
308 conversion range of 5% to 50%. After that, the activation energy declined to lower than zero.

309 The exhaustion of ovalbumin occurred after the conversion rate of 55%. This indicates that
310 the pyrolysis of ovalbumin under CO_2 is more feasible at conversion rate lower than 30%,
311 and the whole process is more efficient compared with N_2 as carrier gas.

312 For spirulina pyrolysis under N_2, the activation energy increased from 160 to 180 kJ/mol (5%
313 $< \alpha <$ 15%) and increased steadily to 190 kJ/mol (20% $< \alpha <$ 50%), after which the value
314 surged to 335 kJ/mol (55% $< \alpha <$ 80%). Similar to the pyrolysis of ovalbumin, the activation
315 energy then decreased dramatically to nearly zero. Since a large proportion of spirulina
316 consists of protein with content of 57.8 wt. %, the activation energy for the pyrolysis of this
317 algae followed a similar trend as shown in ovalbumin under CO_2. This was clear from the
318 increase in E_a during the initial stage from 178 to 317 kJ/mol (5% $< \alpha <$ 55%). It is also
319 obvious that the pyrolysis in CO_2 required higher activation energy compared to N_2 as carrier
320 gas but the pyrolysis in CO_2 proceeded quicker and ended earlier.

321 Overall, by comparing activation energy derived from the pyrolysis of three model
322 compounds under N_2 and CO_2, the ovalbumin required lower amount of energy to
323 decompose and the process proceeded quicker under CO_2 atmosphere. It was found in this
324 study that CO_2 could assist in the pyrolysis of algal protein. Proteins are long chains of
325 polymerized amino acids, also involved in cell structure. There are various species of protein
326 contained in algae, since one single cell produces thousands of different proteins with
327 different amino acid composition. The nitrogen-released compounds are mainly in the form
328 of organic nitrites, nitriles, amines, amides, indoles, pyrroles and their derivatives [42].

However, under CO_2 atmosphere, the activation energy remained relatively unchanged for the pyrolysis of cellulose, while higher activation energy of oil droplet highlighted the difficulty for algal lipid to decompose.

3.2.2 Determination of reaction model via Coats- Redfern method

According to TG/DTG analysis, heating rate affected the pyrolysis process significantly. Due to the severe thermal lag, the kinetic factors calculated based on high heating rates were usually underestimated values as compared to the actual values [43, 44]. The total time for pyrolysis would be reduced by the rising heating rate, so is the period of heat transfer from pan to the sample; thus, the temperature of decomposition will be drifted to higher temperatures. Hence, to minimize the influence of thermal hysteresis, result collected under low pyrolysis heating rate of 5°C/min was used to determine the reaction model. Similar approach was carried out in other open literatures [8, 10]. Commonly-used mechanism models were substituted into Coats-Redfern method to plot $ln\frac{G(\alpha)}{T^2}$ against $-\frac{1}{RT}$ for the major pyrolysis stage. As the temperature increasing, the degradation of samples could be devided into two ranges (Events I and II) under different reaction mechanisms. On the basis of R^2 fitting method, the category of mechanism, activation energy (E_a), and pre-exponential (A) corresponding to the best regression value, among the application of each form, $G(\alpha)$, as shown in **Error! Reference source not found.**.

Table 4 Activation energy, pre-exponential factor and related kinetic models of Events I and II under N_2 and CO_2.

		N_2				CO_2			
	Parameters	**Ovalbumin**	**Cellulose**	**Oil droplet**	**Spirulina**	**Ovalbumin**	**Cellulose**	**Oil droplet**	**Spirulina**
Event I	**Range(°C)**	180-220	300-325	340-440	220-270	180-220	300-325	340-430	220-300
	E_a (kJ/mol)	74.4	273.0	227.8	121.7	66.8	266.6	266.5	20.7
	Mechanism	Second-order reaction (F2)	First-order reaction (F1)	1-D diffusion (D1)	1-D diffusion (D1)	Second-order reaction (F2)	First-order reaction (F1)	2-D diffusion (D2)	1-D diffusion (D1)
	A (s^{-1})	3.3×10^{6}	23.4	1.4×10^{16}	4.6×10^{4}	4.0×10^{5}	22.8	2.29×10^{19}	0.3
Event II	**Range(°C)**	220-400	325-350		270-380	220-400	325-350		300-360
	E_a (kJ/mol)	41.5	377.4		53.0	24.4	344.2		62.1
	Mechanism	Second-order reaction (F2)	Second-order reaction (F2)		Second-order reaction (F2)	Second-order reaction (F2)	Second-order reaction (F2)		Second-order reaction (F2)
	A (s^{-1})	164.7	32.8		4.3×10^{9}	0.6	29.9		4.5

349 According to Figure 4, the activation energy of ovalbumin would increase gradually during
350 the initial decomposition stage and rocketed to high values in the end, which indicated that
351 the two-reaction mechanism dominated this stage of pyrolysis. The carbonaceous matters
352 of ovalbumin were the first to decompose from 180°C, which fitted well with the Second-
353 order chemical reaction (F2) model, and required the lowest activation energy of 74.4
354 kJ/mol. As the pyrolysis temperature increased, the activation energy of ovalbumin in Event
355 II reduced to 41.5 kJ/mol from 220°C, which was much lower than the value derived by KAS
356 method, and the mechanism of ovalbumin pyrolysis remained as F2 model. Cellulose was
357 the second model compound to decompose from 300 to 360°C, which required higher
358 activation energy of the First-order chemical reaction (F1) model (273.0 kJ/mol) in the
359 temperature range of 300-325°C, followed by Event II. From 325 to 350°C, the E_a increased
360 to 377.4 kJ/mol in F2 model. Compared to the results concluded from the KAS method, the
361 activation energy is very different. The E_a decreased from 202.5 to 171.4 kJ/mol during the
362 whole period of pyrolysis and increased to about 198.4 kJ/mol at α=0.95. Similarly, oil
363 droplet did not alter evidently and therefore, one reaction model was used in the pyrolysis
364 process, which appeared to be 1-D diffusion (D1) model. It was the last model substance to
365 decompose at 340 °C until 440 °C with activation energy of 227.8 kJ/mol, which was higher
366 than the value obtained via KAS method (approximately 180kJ/mol). Hence, the protein in
367 algae was the first primary component to decompose during the second stage, followed by
368 carbohydrate which has higher activation energy whilst protein continued to generate
369 volatiles. Lipid in algae was the last component to pyrolyze, which required higher activation
370 energy and decomposed with the remaining carbohydrate and protein, simultaneously.

However, the decomposition of spirulina was found to be in D1 model with an activation energy of 122.6 kJ/mol from 220 to 270°C. After 270°C, the mechanism was changed to F2 model and the E_a required was reduced to an amount of 53.0 kJ/mol.

As for the CO_2 atmosphere, ovalbumin was the first sample to decompose in F2 mechanism which is the same as the decomposition under N_2 with only 66.8 kJ/mol activation energy from 180°C. After 220°C. The activation energy then followed the same decreasing trend in F2 model to 24.4 kJ/mol as N_2 atmosphere. Meanwhile, compared with N_2 atmosphere, cellulose started to decompose in F1 model from 300 to 325°C with similar activation energy (266.6 kJ/mol) and pre-exponential factor (22.8). The E_a further increased to 344.2 kJ/mol in the temperature range of 325 to 350°C in F2 model, which is comparable to the parameters derived under N_2. On the other hand, the oil droplet decomposed with higher activation energy of 266.5 kJ/mol, compared to the value under N_2 atmosphere. Therefore, it is evident that similar decomposition sequence of the three model compounds can be observed under CO_2, compared to N_2 as carrier gas. Moreover, activation energy for the decomposition of the ovalbumin is smaller, which suggests that ovalbumin is easier to decompose in CO_2 atmosphere. As for the lipid, its decomposition occurred at higher temperature with lower degradation rate and higher activation energy, which suggests that it is difficult to decompose in CO_2 atmosphere. This leads to the same conclusion as using KAS method. Spirulina required less energy to proceed the decomposition under CO_2, which decomposed in D1 model with 20.7 kJ/mol for Event I, and switched to F2 mechanism with E_a of 36.4 kJ/mol, compared to the decomposition under N_2 atmosphere.

392 The Coats-Redfern method, which is commonly applied in the determination of reaction
393 mechanism of biomass pyrolysis [45], requires the use of only one set of TG data, while iso-
394 conversional method (KAS) needs at least three sets of data to calculate the thermal
395 parameters. However, different methods are not exclusive, but mutually complementary in
396 the analysis of reaction mechanism [46].

397 **3.3 Characteristics of char**

398 **Error! Reference source not found.** summarizes the composition of char remaining after
399 pyrolysis under N_2 and CO_2 in four different heating rates. As there was minimal char left in
400 the crucibles after pyrolysis of oil droplet (<1wt. %), hence, there are no results for char of
401 algal pseudo- lipid. The compositions of ovalbumin char changed significantly after pyrolysis
402 under N_2 when four different heating rates were used. Carbon and oxygen content of the
403 char fluctuated around 25 and 70 wt. %, respectively. But after pyrolysis in CO_2, the carbon
404 content increased with the increasing of heating rate which then became similar at higher
405 heating rates of 20 and 50 °C/min (14.9 to 22.2 wt.%). This was also observed for the oxygen
406 content (55.9 to 67.6 wt. %). It is apparent that using CO_2 as carrier gas could reduce the
407 carbon and oxygen content in ovalbumin char residue as well as the overall char amount.
408 This reconfirms the previous findings where a smaller activation energy is required for the
409 pyrolysis of ovalbumin in CO_2 as reported in Section 3.2.1. Due to the longer processing time
410 required for lower heating rates (170 mins for 5°C/min, 85 mins for 10 °C/min, 42.5 mins
411 for 20 °C/min and 17 mins for 50°C/min), sample had sufficient time to contact and react
412 with CO_2 via $C+CO_2 \rightarrow 2CO$ reaction. This reduced the carbon content in char significantly,

while increasing the compositions of other elements. Elements including Na, Mg, Si, P, K, and Ca, in the char of ovalbumin pyrolyzed under CO_2 increased steadily as the heating rate was reduced. At the heating rate of 5 °C/min, these elements were significantly larger than the amount derived under N_2, especially for P, K, Ca, and Mg at 8.0, 10.3, 1.6 and 2.1 wt. %, respectively.

Table 5 Elemental compositions of solid residues of ovalbumin, cellulose and spirulina derived by EDS.

Ovalbumin												
Heating rate (°C/min)	N_2				CO_2				Char (CO_2)			
	5	10	20	50	5	10	20	50	5	10	20	50
C	25.4	25.6	25.6	25.5	14.9	20.0	22.2	22.2	15.1	28.6	29.6	29.0
N	-	-	0.4	0.3	-	0.9	0.9	1.7	-	-	-	-
Na	-	-	-	-	0.3	-	-	-	9.5	7.2	5.7	5.3
Mg	0.4	0.4	0.4	0.3	2.1	0.9	0.5	0.4	6.3	6.8	4.4	4.5
Si	-	-	-	-	0.1	-	-	-	-	0.1	0.1	-
P	1.4	1.2	1.2	1.0	8.0	2.8	2.2	1.5	13.2	11.9	9.6	11.6
S	-	-	-	0.1	-	-	-	-	-	-	-	-
Cl	-	-	-	-	-	0.1	-	-	-	-	-	-
K	2.2	2.1	1.8	1.4	10.3	4.5	3.6	1.8	0.3	0.4	0.4	0.6
Ca	0.4	0.2	0.2	0.2	1.6	0.4	0.7	0.2	11.6	11.9	12.9	16.5
Fe	-	-	-	0.1	-	-	-	-	0.2	0.6	0.2	0.3
O	70.3	70.5	70.6	70.8	55.9	62.9	66.4	67.6	43.0	31.8	36.6	31.6
Cellulose												
Heating rate (°C/min)	N_2				CO_2				Char (CO_2)			
	5	10	20	50	5	10	20	50	5	10	20	50
C	27.3	27.3	27.3	27.3	27.3	27.3	27.3	27.3	92.9	90.5	94.3	94.0
O	72.7	72.7	72.7	72.7	72.7	72.7	72.7	72.7	7.1	9.5	5.7	6.0
Spirulina												
Heating rate (°C/min)	N_2				CO_2				Char (CO_2)			
	5	10	20	50	5	10	20	50	5	10	20	50
C	25.4	23.1	24.1	25.0	3.7	15.2	23.8	24.5	2.0	7.7	9.2	9.1
N	-	-	0.7	0.8	-	-	-	-	-	-	-	-
Na	0.4	0.5	0.6	0.4	2.5	1.7	0.8	0.7	4.7	2.6	4.3	2.9
Mg	0.5	0.8	0.6	0.4	4.5	2.3	0.8	0.7	5.9	6.8	4.8	4.9
Al	0.1	0.3	0.3	0.2	3.0	0.9	0.6	0.1	2.2	1.8	2.9	3.1
Si	0.4	0.4	0.2	0.2	2.8	1.0	0.9	0.3	5.2	2.5	5.4	4.1

P	1.4	2.5	1.2	0.9	14.9	5.9	1.8	1.3	13.1	12.1	11.2	11.6
S	0.1	0.1	-	-	-	0.1	0.1	-	-	0.1	-	-
Cl	-	-	-	-	-	0.1	-	-	0.1	-	-	-
K	0.9	1.5	1.0	0.8	13.7	7.0	1.8	1.6	9.4	9.7	7.7	10.3
Ca	0.3	2.1	0.7	0.2	3.4	2.0	0.8	0.4	5.2	10.4	4.2	6.7
Fe	0.1	1.0	0.3	0.4	3.6	1.8	1.1	0.4	4.2	5.6	3.0	4.3
O	70.8	67.8	70.2	70.9	45.2	56.3	68.0	69.8	47.7	34.4	47.3	42.8

As for the cellulose, the elements in char remained relatively the same for both N_2 and CO_2 atmospheres even in various heating rates (carbon, 27.3 wt.%; oxygen, 72.7 wt.%). This also corresponded to the relatively unchanged activation energy calculated in Section 3.2.1. This also indicated that CO_2 minimally participated in the pyrolysis of carbohydrate contained in algae.

Similar to the composition of ovalbumin char, C and O content of spirulina char under four heating rates varied around 25 and 70 wt.% in N_2. However, char derived in CO_2 contained increased amount of carbon and oxygen as the heating rates became larger from 5 to 50 °C/min (3.7 to 24.5 wt.% and 45.2 to 69.8 wt. % respectively). At heating rate of 5 °C/min, elements of char obtained in CO_2, including P, K, Na, Mg, Al, Si, Ca, and Fe were significantly larger than the amount derived in N_2, especially for P and K with 14.9 and 13.7 wt. %, respectively.

The different heating rates have significant influences on the carbon content in char since the CO_2 atmosphere could improve the cracking of VOCs and the reaction between VOCs and CO_2. The carbon content will increase with the increment of heating rate. In order to investigate the effects of processing time on carbon content of solid residue, the pyrolysis of char which was carried out in the tube furnace (using a simulated TGA process at 5 °C/min)

was conducted under four heating rates in CO_2 atmosphere. As the heating rate increased from 5 to 50 °C/min, the carbon content of cellulose char remained steady at around 93 wt. %, which suggested that CO_2 minimally affected the pyrolysis of algal carbohydrate. On the other hand, the carbon content of the newly-prepared char from ovalbumin increased from 15.1 to 29.0 wt. %. This indicated that CO_2 atmosphere would participate in the reaction with carbon contained in char as the pyrolysis progressed, mainly due to the gasification of CO_2 and carbon content.

4 Conclusions

Pyrolysis characteristics of three algal model compounds (cellulose, ovalbumin, oil droplet) and algae (spirulina) were investigated by TGA and analyzed using model free (KAS) and model fitting (Coats-Redfern) methods. It was found that pyrolysis was more efficient at lower heating rates. The algal protein was the first to decompose with the lowest activated energy, followed by carbohydrate and lipid contained in algae. Moreover, CO_2 atmosphere favored the pyrolysis of protein due to the improved cracking of VOCs in ovalbumin as well as the reaction between VOCs and CO_2. However, the decomposition of lipid and carbohydrate was less feasible in CO_2 atmosphere.

Acknowledgement

Following funding bodies are acknowledged for their financial support to this study, National Key R&D Programme (2017YFB0602601), the Natural Science Foundation China (the Young Scientist Fund) [grant number 5160060426] and Ningbo Bureau of Science and Technology (the Innovation Team Scheme) [grant number 2012B82011]. The International

Doctoral Innovation Centre is also acknowledged for the provision of a full scholarship to the first author.

Reference

[1] J. Yan, K. Shi, C. Pang, E. Lester, T. Wu, Influence of minerals on the thermal processing of bamboo with a suite of carbonaceous materials, Fuel 180 (2016) 256-262.

[2] R. Zhang, L. Li, D. Tong, C. Hu, Microwave-enhanced pyrolysis of natural algae from water blooms, Bioresource Technology 212 (2016) 311-317.

[3] Q. Xie, M. Addy, S. Liu, B. Zhang, Y. Cheng, Y. Wan, Y. Li, Y. Liu, X. Lin, P. Chen, R. Ruan, Fast microwave-assisted catalytic co-pyrolysis of microalgae and scum for bio-oil production, Fuel 160 (2015) 577-582.

[4] D. Beneroso, J.M. Bermudez, A. Arenillas, J.A. Menendez, Microwave pyrolysis of microalgae for high syngas production, Bioresource Technology 144 (2013) 240-246.

[5] L. Rodolfi, G. Zittelli, N. Bassi, G. Padovani, N. Biondi, G. Bonini, M. Tredici, Microalgae for Oil: Strain Selection, Induction of Lipid Synthesis and Outdoor Mass Cultivation in a Low-Cost Photobioreactor, Biotechnology & Bioengineering 102(1) (2009) 100-112.

[6] Y. Hong, W. Chen, X. Luo, C. Pang, E. Lester, T. Wu, Microwave-enhanced pyrolysis of macroalgae and microalgae for syngas production, Bioresource Technology 237 (2017) 47-56.

[7] R. Sharma, P.N. Sheth, A.M. Gujrathi, Kinetic modeling and simulation: Pyrolysis of Jatropha residue de-oiled cake, Renewable Energy 86 (2016) 554-562.

[8] S. Wang, H. Lin, B. Ru, G. Dai, X. Wang, G. Xiao, Z. Luo, Kinetic modeling of biomass components pyrolysis using a sequential and coupling method, Fuel 185 (2016) 763-771.

[9] A. Zaker, Z. Chen, X. Wang, Q. Zhang, Microwave-assisted pyrolysis of sewage sludge: A review, Fuel Processing Technology 187 (2019) 84-104.

[10] R. Maurya, T. Ghosh, H. Saravaia, C. Paliwal, A. Ghosh, S. Mishra, Non-isothermal pyrolysis of de-oiled microalgal biomass: Kinetics and evolved gas analysis, Bioresource Technology 221 (2016) 251-261.

[11] S. Vyazovkin, A unified approach to kinetic processing of nonisothermal data, International Journal of Chemical Kinetics 28(2) (1996) 95-101.

[12] M. Hu, X. Wang, J. Chen, P. Yang, C. Liu, B. Xiao, D. Guo, Kinetic study and syngas production from pyrolysis of forestry waste, Energy Conversion and Management 135 (2017) 453-462.

[13] S. Vyazovkin, A.K. Burnham, J.M. Criado, L.A. Pérez-Maqueda, C. Popescu, N. Sbirrazzuoli, ICTAC Kinetics Committee recommendations for performing kinetic computations on thermal analysis data, Thermochimica Acta 520(1–2) (2011) 1-19.

[14] S. Ceylan, D. Kazan, Pyrolysis kinetics and thermal characteristics of microalgae Nannochloropsis oculata and Tetraselmis sp, Bioresource Technology 187 (2015) 1-5.

[15] S. Ceylan, Y. Topcu, Z. Ceylan, Thermal behaviour and kinetics of alga Polysiphonia elongata biomass during pyrolysis, Bioresource Technology 171(1) (2014) 193-198.
[16] C. Gai, Y. Zhang, W.T. Chen, P. Zhang, Y. Dong, Thermogravimetric and kinetic analysis of thermal decomposition characteristics of low-lipid microalgae, Bioresource Technology 150(3) (2013) 139-148.
[17] J. Lee, J.-I. Oh, Y.S. Ok, E.E. Kwon, Study on susceptibility of CO2-assisted pyrolysis of various biomass to CO2, Energy 137 (2017) 510-517.
[18] L. Tang, Y. Yan, Y. Meng, J. Wang, P. Jiang, C.H. Pang, T. Wu, CO2 gasification and pyrolysis reactivity evaluation of oil shale, Energy Procedia 158 (2019) 1694-1699.
[19] L. Li, R. Zhang, D. Tong, C. Hu, Fractional Pyrolysis of Algae and Model Compounds†, Chinese Journal of Chemical Physics 28(4) (2015) 525-532.
[20] M.T. Cesário, M.M.R. da Fonseca, M.M. Marques, M.C.M.D. de Almeida, Marine algal carbohydrates as carbon sources for the production of biochemicals and biomaterials, Biotechnology Advances 36(3) (2018) 798-817.
[21] L. Sheng, X. Wang, X. Yang, Prediction model of biocrude yield and nitrogen heterocyclic compounds analysis by hydrothermal liquefaction of microalgae with model compounds, Bioresource Technology 247 (2018) 14-20.
[22] T. Wu, M. Gong, E. Lester, F. Wang, Z. Zhou, Z. Yu, Characterisation of residual carbon from entrained-bed coal water slurry gasifiers, Fuel 86(7–8) (2007) 972-982.
[23] J. Oladejo, S. Adegbite, X. Gao, H. Liu, T. Wu, Catalytic and non-catalytic synergistic effects and their individual contributions to improved combustion performance of coal/biomass blends, Applied Energy 211 (2018) 334-345.
[24] A.M. Parvez, T. Wu, Characteristics and interactions between coal and carbonaceous wastes during co-combustion, Journal of the Energy Institute 90(1) (2017) 12-20.
[25] A.M. Parvez, Y. Hong, E. Lester, T. Wu, Enhancing the Reactivity of Petroleum Coke in CO2 via Co-Processing with Selected Carbonaceous Materials, Energy and Fuels 31(2) (2017) 1555-1563.
[26] A.C.R. Lim, B.L.F. Chin, Z.A. Jawad, K.L. Hii, Kinetic Analysis of Rice Husk Pyrolysis Using Kissinger-Akahira-Sunose (KAS) Method , Procedia Engineering 148 (2016) 1247-1251.
[27] I. Ali, S.R. Naqvi, A. Bahadar, Kinetic analysis of Botryococcus braunii pyrolysis using model-free and model fitting methods, Fuel 214 (2018) 369-380.
[28] L. Tian, A. Tahmasebi, J. Yu, An experimental study on thermal decomposition behavior of magnesite, Journal of Thermal Analysis & Calorimetry 118(3) (2014) 1577-1584.

[29] S.Y. Yorulmaz, A.T. Atimtay, Investigation of combustion kinetics of treated and untreated waste wood samples with thermogravimetric analysis, Fuel Processing Technology 90(7-8) (2009) 939-946.
[30] Q.V. Bach, W.H. Chen, A comprehensive study on pyrolysis kinetics of microalgal biomass, Energy Conversion & Management 131 (2017) 109-116.
[31] W.P. Chan, J.-Y. Wang, Characterisation of sludge for pyrolysis conversion process based on biomass composition analysis and simulation of pyrolytic properties, Waste Management 72 (2018) 274-286.
[32] W.P. Chan, J.-Y. Wang, Formation of synthetic sludge as a representative tool for thermochemical conversion modelling and performance analysis of sewage sludge – Based on a TG-FTIR study, Journal of Analytical and Applied Pyrolysis 133 (2018) 97-106.
[33] S.R. Naqvi, R. Tariq, Z. Hameed, I. Ali, M. Naqvi, W.-H. Chen, S. Ceylan, H. Rashid, J. Ahmad, S.A. Taqvi, M. Shahbaz, Pyrolysis of high ash sewage sludge: Kinetics and thermodynamic analysis using Coats-Redfern method, Renewable Energy 131 (2019) 854-860.
[34] A. Plis, J. Lasek, A. Skawińska, J. Zuwała, Thermochemical and kinetic analysis of the pyrolysis process in Cladophora glomerata algae, Journal of Analytical & Applied Pyrolysis 115 (2015) 166-174.
[35] P. Giudicianni, G. Cardone, R. Ragucci, Cellulose, hemicellulose and lignin slow steam pyrolysis: Thermal decomposition of biomass components mixtures, Journal of Analytical and Applied Pyrolysis 100 (2013) 213-222.
[36] X. Dai, C. Wu, L. Haibin, Y. Chen, The Fast Pyrolysis of Biomass in CFB Reactor, Energy & Fuels 14(3) (2000) 552-557.
[37] R. Comesaña, M.A. Gómez, M.A. Álvarez, P. Eguía, Thermal lag analysis on a simulated TGA-DSC device, Thermochimica Acta 547 (2012) 13-21.
[38] A.I. Casoni, J. Zunino, M.C. Piccolo, M.A. Volpe, Valorization of Rhizoclonium sp. algae via pyrolysis and catalytic pyrolysis, Bioresource Technology 216 (2016) 302-307.
[39] N. Sbirrazzuoli, L. Vincent, A. Mija, N. Guigo, Integral, differential and advanced isoconversional methods : Complex mechanisms and isothermal predicted conversion–time curves, Chemometrics & Intelligent Laboratory Systems 96(2) (2009) 219-226.
[40] W.P. Chan, J.Y. Wang, Comparison study on thermal degradation behaviours and product distributions for various types of sludge by using TG-FTIR and fixed bed pyrolysis, Journal of Analytical & Applied Pyrolysis 121 (2016) 177-189.
[41] D.L. Urban, M.J.A. Jr, Study of the kinetics of sewage sludge pyrolysis using DSC and TGA, Fuel 61(9) (1982) 799-806.

[42] P.E. Amaral Debiagi, M. Trinchera, A. Frassoldati, T. Faravelli, R. Vinu, E. Ranzi, Algae Characterization and Multistep Pyrolysis Mechanism, Journal of Analytical and Applied Pyrolysis (2017).
[43] R.N. And, M.J. Antal, Thermal Lag, Fusion, and the Compensation Effect during Biomass Pyrolysis†, Industrial & Engineering Chemistry Research 35(5) (1996) 1711-1721.
[44] M. Grønli, M.J. Antal, G. Várhegyi, A Round-Robin Study of Cellulose Pyrolysis Kinetics by Thermogravimetry, Industrial & Engineering Chemistry Research 38(6) (1999) 2238-2244.
[45] W. Gao, K. Chen, J. Zeng, J. Xu, B. Wang, Thermal pyrolysis characteristics of macroalgae Cladophora glomerata, Bioresource Technology 243 (2017) 212-217.
[46] S. Feng, P. Li, Z. Liu, Y. Zhang, Z. Li, Experimental study on pyrolysis characteristic of coking coal from Ningdong coalfield, Journal of the Energy Institute 91(2) (2018) 233-239.